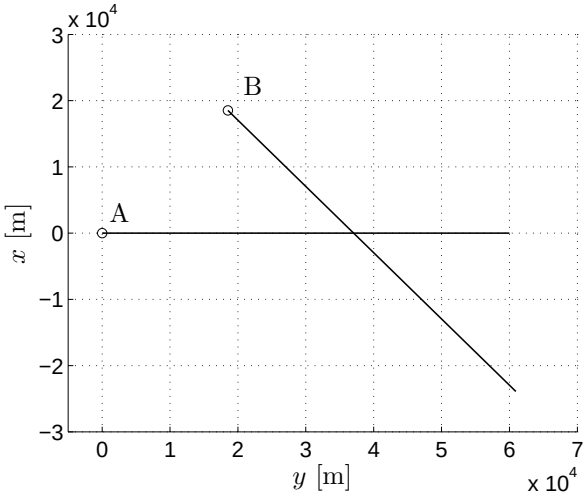

Figure 3. Aircraft trajectories.

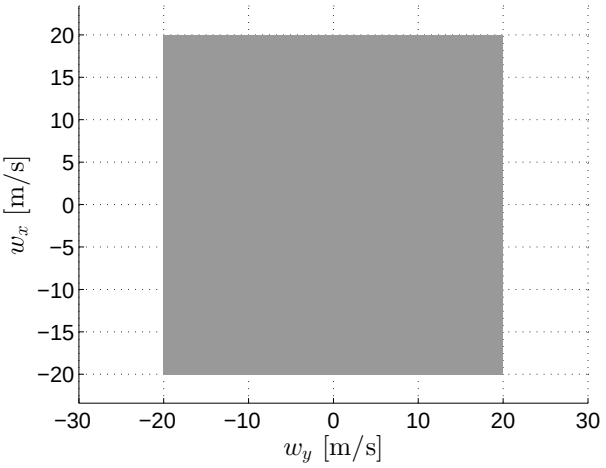

Figure 4. Two-dimensional set in the $w_x w_y$-plane, for $\bar{w} = 0$ and $\delta_w = 20$ m/s.

Next, results are presented for each indicator. All the results are validated by the Monte Carlo method; the number of samples for each simulation (i.e., for each value of $\bar{w}$ and δ_w) is 2^{23} (aprox. 8.4 million). The probability of having an error on the mean value of an indicator obtained by the Monte Carlo method, $\bar{v}_1$, larger than some given tolerance, ε, can be estimated as (see Bayer et al. [15])

$$P[|\bar{v}_1 - E[v_1]| > \varepsilon] \approx 2\left(1 - \Phi\left[\frac{\sqrt{N}\varepsilon}{\sigma[v_1]}\right]\right), \qquad (18)$$

where N is the number of samples and Φ is the standard normal cumulative distribution function. As a reference, for $\bar{w} = 0$, $\delta_w = 20$ m/s, and the chosen number of samples $N = 2^{23}$, the probability of having an error larger than 1 m in the mean value of d_{min} is 0.71%. As it will be seen in all cases, the results obtained with the Monte Carlo method are almost indistinguishable from those obtained with the transformation method.

A. *Minimum distance, d_{min}*

Initially, results are presented for $\bar{w} = 0$ and $\delta_w = 20$ m/s. The two-dimensional set R_{w_x,w_y} and its transformation onto the $d_{min}w_y$-plane, R_{d_{min},w_y}, are presented in Figs. 4 and 5, respectively. The PDF of d_{min} is shown in Fig. 6. The existence of the four corners of the PDF (at 7.5, 9.0, 11.0, and 12.4 km approximately, labeled as c, d, b, and a, respectively) can be explained by the four corners of R_{d_{min},w_y} (labeled with the same letters): when the marginal PDF is obtained by integrating on w_y, these corners represent abrupt changes in the integration limits.

The expected value and the standard deviation of d_{min} are 10012 and 1076 m, respectively (10013 and 1076 m with Monte Carlo method). The probability of conflict is $P_{con} = 28.0\%$, which is obtained as the area under the PDF to the left of the vertical line that represents the separation minimum D (vertical dash-dot line in Fig. 6).

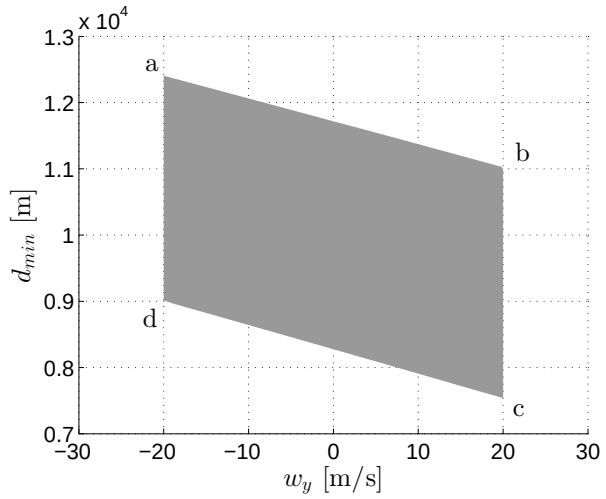

Figure 5. Two-dimensional set in the $d_{min}w_y$-plane, for $\bar{w} = 0$ and $\delta_w = 20$ m/s.

Next, results are presented for different values of the mean wind $\bar{w}$ and the width δ_w. In Fig. 7 it can be seen that the expected value $E[d_{min}]$ does not depend on δ_w and decreases as $\bar{w}$ increases. Since $E[d_{min}]$ does not depend on δ_w, its evolution with $\bar{w}$ can be explained considering the deterministic case (i.e., $\delta_w = 0$): as $\bar{w}$ increases the wind changes from pointing Southwest to pointing Northeast; both airspeeds $\vec{V}_A$ and $\vec{V}_B$ rotate clockwise to keep their course constant, being aircraft B more affected by the wind because the wind direction is entirely perpendicular to its course; as a result, $\vec{V}_g$ also rotates clockwise (see Fig. 8), being more aligned with $\vec{s}_0$; hence, the term $\left(\vec{s}_0\vec{V}_g\right)^2/V_g^2$ increases and thus d_{min} decreases.

The standard deviation $\sigma[d_{min}]$ is shown in Fig. 9. As expected, it increases as δ_w increases; as a numerical reference,

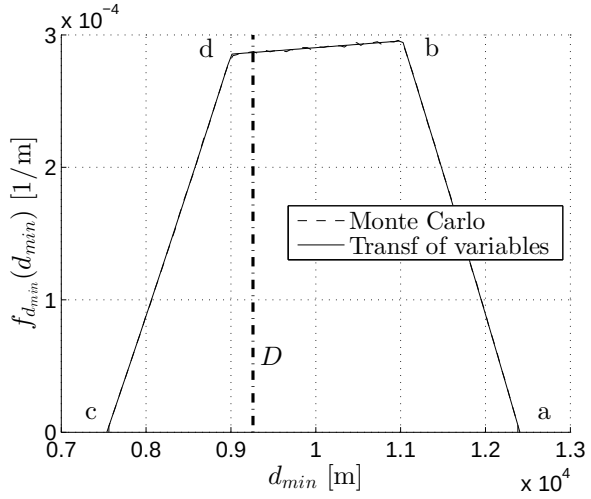

Figure 6. PDF of d_{min}, for $\bar{w} = 0$ and $\delta_w = 20$ m/s.

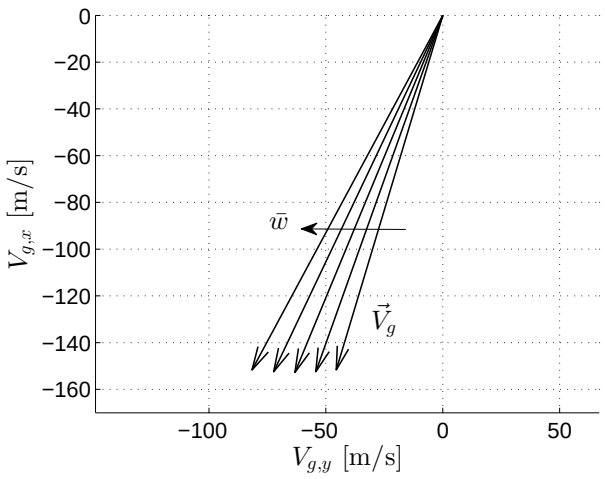

Figure 8. $\vec{V}_g$ for $\bar{w} = -20, -10, 0, 10, 20$ m/s and $\delta_w = 0$.

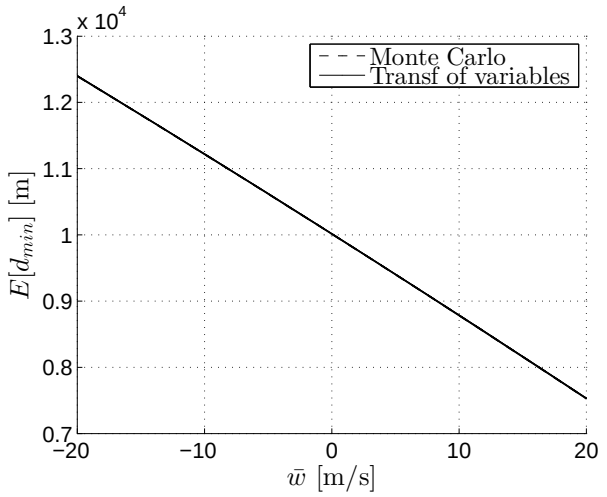

Figure 7. Expected value of d_{min} as a function of $\bar{w}$, for $\delta_w = 5, 10, 15, 20, 25$ m/s.

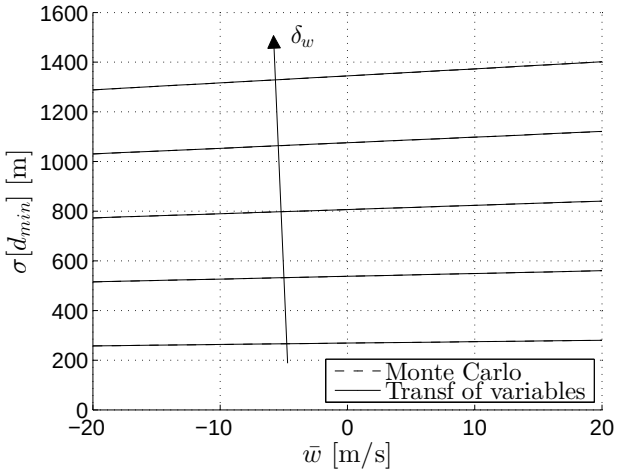

Figure 9. Standard deviation of d_{min} as a function of $\bar{w}$, for $\delta_w = 5, 10, 15, 20, 25$ m/s.

for $\bar{w} = 0$ it increases 54 m when δ_w increases 1 m/s. Its dependence with $\bar{w}$ is very weak, increasing very slightly.

B. Time to minimum distance, $t_{d_{min}}$

The $R_{t_{d_{min}},w_y}$ region and the PDF of $t_{d_{min}}$ are depicted in Figs. 10 and 11, respectively, for $\bar{w} = 0$ and $\delta_w = 20$ m/s. As in the case of d_{min}, the PDF shows four corners, two of them very close to each other (at approximately 130 s) and hard to distinguish; as in the case of d_{min}, the existence of these corners can be explained by the four corners of $R_{t_{d_{min}},w_y}$. The expected value and the standard deviation are 131.9 and 6.4 s, respectively (same values are obtained with Monte Carlo method).

The evolution of the expected value $E[t_{d_{min}}]$ and the standard deviation $\sigma[t_{d_{min}}]$ with the mean wind $\bar{w}$ and the width δ_w is shown in Figs. 12 and 13, respectively. It can be seen that $E[t_{d_{min}}]$ is almost independent of both wind parameters, and that $\sigma[t_{d_{min}}]$ depends very weakly on $\bar{w}$ (it decreases very slightly). As in the case of d_{min}, the evolution of the expected value can be analized considering the deterministic case: as $\bar{w}$ increases $\vec{V}_g$ rotates clockwise and its magnitude also increases (see Fig. 8), the term $\left(\vec{s}_0 \vec{V}_g\right)/V_g^2$ happens to remain approximately constant. Obviously, this result pertains to the particular scenario considered in this paper and cannot be generalized.

As expected, $\sigma[t_{d_{min}}]$ increases as δ_w increases. As a numerical reference, for $\bar{w} = 0$, $\sigma[t_{d_{min}}]$ increases 0.3 s when δ_w increases 1 m/s. Its dependence with $\bar{w}$ is very weak, decreasing very slightly.

C. Probability of conflict, P_{con}

The probability of conflict P_{con} is shown in Fig. 14 for different values of $\bar{w}$ and δ_w. In this figure, the deterministic case has been also included ($\delta_w = 0$) as a reference; it is

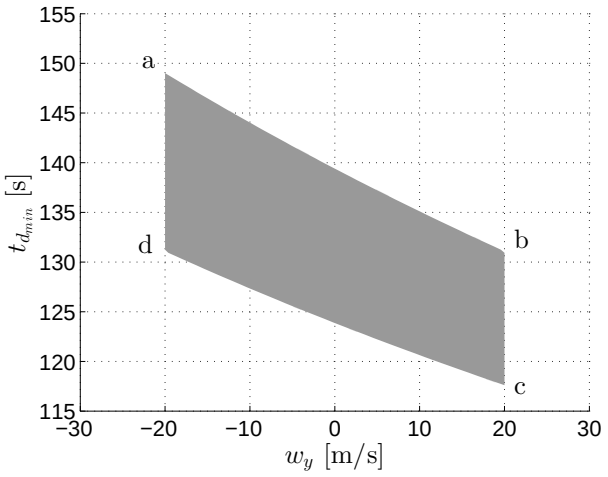

Figure 10. Two-dimensional set in the $t_{d_{min}} w_y$-plane, for $\bar{w} = 0$ and $\delta_w = 20$ m/s.

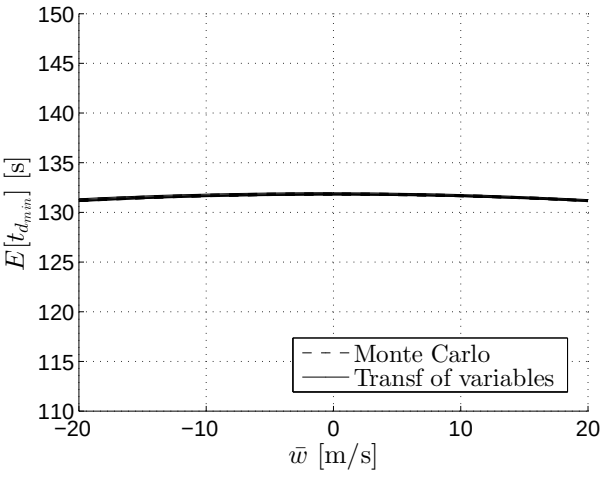

Figure 12. Expected value of $t_{d_{min}}$ as a function of $\bar{w}$, for $\delta_w = 5, 10, 15, 20, 25$ m/s.

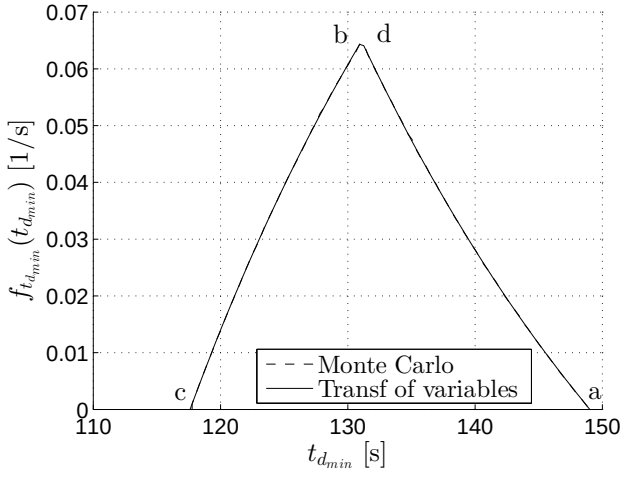

Figure 11. PDF of $t_{d_{min}}$, for $\bar{w} = 0$ and $\delta_w = 20$ m/s.

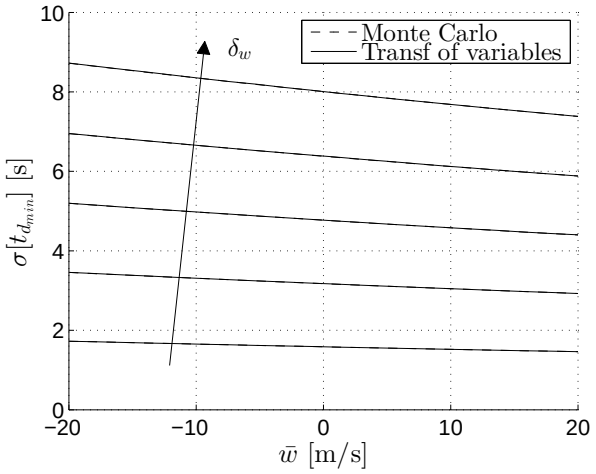

Figure 13. Standard deviation of $t_{d_{min}}$ as a function of $\bar{w}$, for $\delta_w = 5, 10, 15, 20, 25$ m/s.

represented by the line that changes instantly from 0 to 100 % probability at $\bar{w} = 6.2$ m/s. It can be seen that for large negative values of $\bar{w}$ and any value of δ_w the probability is nil ($P_{con} = 0$) because the minimum distance between aircraft is large (see Fig. 7). As $\bar{w}$ increases, P_{con} increases because the minimum distance decreases, and at some point the conflict becomes certain ($P_{con} = 100$ %).

P_{con} can decrease or increase as δ_w increases, depending on the value of $\bar{w}$. In this application, it has been found that, when no conflict exists in the deterministic case ($\bar{w} < 6.2$ m/s), an increase of the wind uncertainty results in a higher probability of having winds which can result into a conflict, thus increasing P_{con}. On the contrary, when a conflict exists in the deterministic case ($\bar{w} > 6.2$ m/s), as the wind uncertainty increases, a higher probability of having winds which do not result into a conflict also increases, thus reducing P_{con}. In both cases, the certainty that a conflict does exist or does not exist decreases as the wind uncertainty increases.

VI. Conclusions

The general framework for this paper is the development of a methodology to manage weather uncertainty suitable to be integrated into the traffic management process. This work is a first step focused on the assessment of the impact of wind uncertainty on conflict detection, and in particular on the en-route phase of flight. The methodology presented in this work allows to assess the probability of conflict in given scenarios and other uncertain characteristics of the conflict. It is expected that by considering the weather uncertainty in the trajectory prediction process, the safety and efficiency of the air traffic may be improved by strategically deconflicting the trajectories and by reducing the number of missed and false alerts.

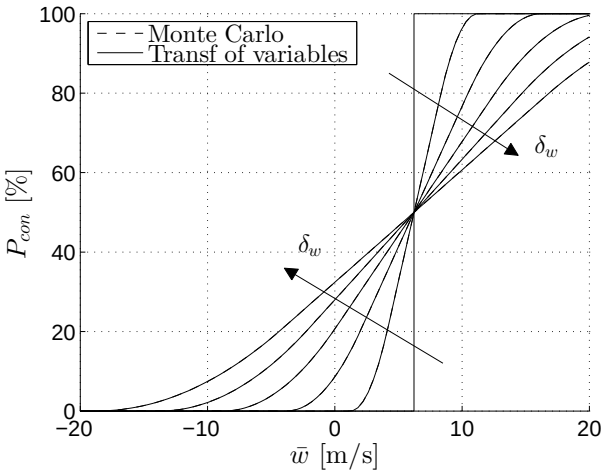

Figure 14. Probability of conflict as a function of $\bar{w}$, for $\delta_w = 0, 5, 10, 15, 20, 25$ m/s.

The probabilistic approach presented in this paper is capable of taking as input any type of wind distribution derived from ensemble weather forecasts. In this work, a simple uniform distribution has been considered in the numerical application. The determination of the wind probability density function from the uncertainty information contained in the ensemble forecast is an open challenge in this problem.

In this paper, the minimum distance between aircraft, the time to minimum distance, and the conflict probability have been chosen to describe the conflict. Under the hypotheses that the aircraft follow a constant course and they are affected by the same wind, it has been found that these three indicators depend on the crosswinds seen by both aircraft, but not on the along-track winds. As an interesting result, if the trajectories are only affected by along-track winds then these conflict indicators result to be certain.

The influence of the wind uncertainty on the conflict indicators have beed assessed using the methodology of transformation of random variables. This methodology allows to obtain the probability density functions of the conflict indicators, and therefore their expected values, standard deviations or associated probabilities. This same methodology could be applied to other indicators to describe other characteristics of the conflict, e.g. indicators related to the time instant at which the loss of separation starts, the duration of the loss of separation, or the probability for each aircraft of being in loss of separation at a given position along the trajectory.

Some numerical results have been presented for a particular scenario to show the potentiality of the proposed methodology. The effects of the average wind and the wind dispersion on the conflict indicators have been shown.

Next steps in this research are the obtention of wind distributions from actual ensemble forecasts and the application of the probabilistic approach presented in this paper to trajectories composed of several cruise segments with different courses. Also for future work is left the task of considering each aircraft affected by a different wind obtained from a statistically-correlated wind-field.

Acknowledgements

The authors gratefully acknowledge the financial support of the Spanish Ministerio de Economía y Competitividad through Grant TRA2014-58413-C2-1-R, co-financed with FEDER funds.

References

[1] D. Rivas and R. Vazquez, "Uncertainty," in Complexity Science in Air Traffic Management, A. Cook and D. Rivas Ed., Ashgate Publishing Limited, 2016, Chap. 4.

[2] Q.M. Zheng and Y.J. Zhao, "Modeling Wind Uncertainties for Stochastic Trajectory Synthesis," 11th AIAA Aviation Technology, Integration, and Operations (ATIO) Conference, paper AIAA 2011-6858, 2011, pp. 1–10.

[3] A. Nilim, L. El Ghaoui, M. Hansen, and V. Duong, "Trajectory-based Air Traffic Management (TB-ATM) under Weather Uncertainty," Proc. 4th USA/Europe Air Traffic Management Research and Development Seminar (ATM-2001), Santa Fe, NM, 2001, pp. 1–11.

[4] D. Gonzalez Arribas, M. Soler Arnedo, and M. Sanjurjo Rivo, "Wind-optimal Cruise Trajectories using Pseudospectral Methods and Ensemble Probabilistic Forecasts," Proc. 5th International Conference on Application and Theory of Automation in Command and Control Systems (ATACCS2015), Toulouse, France, 2015, pp. 1–8.

[5] M. Steiner, C.K. Mueller, G. Davidson, and J.A. Krozel, "Integration of Probabilistic Weather Information with Air Traffic Management Decision Support Tools: A conceptual Vision for the Future," 13th Conference on Aviation, Range and Aerospace Meteorology, New Orleans, LA, 2008, pp. 1–9.

[6] D. Rivas, R. Vazquez, and A. Franco, "Probabilistic Analysis of Aircraft Fuel Consumption using Ensemble Weather Forecasts," 7th International Conference on Research in Air Transportation (ICRAT), Philadelphia, PA, 2016, pp. 1–8.

[7] R.A. Paielli and H. Erzberger, "Conflict Probability Estimation for Free Flight," *Journal of Guidance, Control, and Dynamics*, Vol. 20, no. 3, 1997, pp. 588–596.

[8] M. Prandini, J. Hu, J. Lygeros, and S. Sastry, "A Probabilistic Approach to Aircraft Conflict Detection," *IEEE Transactions on Intelligent Transportation Systems*, Vol. 1, No. 4, 2000, pp. 199–220.

[9] J. Hu, M. Prandini, and S. Sastry, "Aircraft Conflict Prediction in the Presence of a Spatially Correlated Wind Field," *IEEE Transactions on Intelligent Transportation Systems*, Vol. 6, No. 3, 2005, pp. 326–340.

[10] R.V. Hogg and A.T. Craig, "Introduction to Mathematical Statistics," Prentice-Hall International, Englewood Cliffs, N.J., 1995, pp. 168–178.

[11] World Meteorological Organization, "Guidelines on Ensemble Prediction Systems and Forecasting," WMO-No. 1091, 2012.

[12] J.Cheung, A. Hally, J. Heijstek, A. Marsman, and J.-L. Brenguier, "Recommendations on Trajectory Selection in Flight Planning based on Weather Uncertainty," Proc. 5th SESAR Innovation Days (SID2015), Bologna, Italy, 2015, pp. 1–8.

[13] "IMET - Investigating the optimal approach for future trajectory prediction (TP) systems to use METeorological uncertainty information. SESAR WP-E Project 02.40," Poster in 3rd SESAR Innovation Days (SID2013), Stockholm, Sweden, 2013. [Online] Available: http://sesarinnovationdays.eu/files/2013/Posters/SID%202013%20poster%20IMET.pdf

[14] T. Gneiting, "Calibration of Medium-Range Weather Forecasts," European Centre for Medium-Range Weather Forecasts, 2014.

[15] C. Bayer, H. Hoel, E. von Schwerin, and R. Tempone, "On Nonasymptotic Optimal Stopping Criteria in Monte Carlo Simulations," *SIAM Journal on Scientific Computing*, Vol. 36, No. 2, pp. A869–A885, 2014.